Simultaneously Targeting Myofibroblast Contractility and Extracellular Matrix Cross-Linking as a Therapeutic Concept in Airway Fibrosis

Yu-chun Lin[1,2], **Yon K. Sung**[2], **Xinguo Jiang**[1,2], **Marc Peters-Golden**[3], and **Mark R. Nicolls**[1,2,*]

[1] Division of Pulmonary and Critical Care Medicine, Department of Medicine, Stanford University, Stanford, California; USA

[2] Veterans Affairs Palo Alto Health Care System, Palo Alto, California, USA

[3] Division of Pulmonary and Critical Care Medicine, Department of Medicine, University of Michigan, Ann Arbor, Ann Arbor, Michigan, USA

Abstract

Fibrosis after solid organ transplantation is considered an irreversible process and remains the major cause of graft dysfunction and death with limited therapies. This remodeling is characterized by aberrant accumulation of contractile myofibroblasts that deposit excessive extracellular matrix (ECM) and increase tissue stiffness. However, studies demonstrate that a stiff ECM, itself, promotes fibroblast-to-myofibroblast differentiation, stimulating further ECM production. This creates a positive feedback loop that perpetuates fibrosis. We hypothesized that simultaneously targeting myofibroblast contractility with relaxin and ECM stiffness with lysyl oxidase inhibitors could break the feedback loop, thereby, reversing established fibrosis.

To test this, we used the orthotopic tracheal transplanted (OTT) mouse model, which develops robust fibrotic airway remodeling. Mice with established fibrosis were treated with saline, mono-, or combination therapies. While monotherapies had no effect, combining these agents decreased collagen deposition and promoted re-epithelialization of remodeled airways. Relaxin inhibited myofibroblast differentiation and contraction, in a matrix-stiffness-dependent manner through prostaglandin E_2 (PGE_2). Furthermore, the effect of combination therapy was lost in PGE_2 receptor knockout and PGE_2 inhibited OTT mice. This study reveals the important synergistic roles of cellular contractility and tissue stiffness in the maintenance of fibrotic tissue and suggests a new therapeutic principle for fibrosis.

---

*Corresponding author: Mark R. Nicolls, MD, Division of Critical Care Medicine, Department of Medicine, Stanford University, VA Palo Alto Health Care System, Medical Service 111P, 3801 Miranda Ave. Palo Alto, CA 94304 mnicolls@stanford.edu.

Introduction

After tissue injury, the reparative response is characterized by a transient appearance of myofibroblasts that produce provisional, collagenous scars which protect against further damage and rupture. In a normal response, the provisional scars are eventually replaced by normal tissue. In fibrosis, however, there is persistent accumulation and activation of myofibroblasts, resulting in over-production of stiff ECM that replaces the normal tissue. Because there are few therapeutic options for reversing fibrosis, this process may cause organ dysfunction and death. Previous studies have demonstrated that the increased ECM stiffness that occurs in fibrosis is not only a consequence of myofibroblast activation but also a causative factor that independently perpetuates fibrosis (1, 2). The mechanical resistance of the ECM stimulates myofibroblasts to express α-smooth muscle actin (α-SMA) which enables cell contraction. This cellular conversion then triggers the secretion and activation of cytokines and growth factors leading to additional ECM production creating a positive feedback loop (3).

Recent anti-fibrotic strategies targeting myofibroblast differentiation and contraction have shown promising results (4). Among these approaches is the use of relaxin. Relaxin appears to inhibit fibrosis by attenuating cellular contraction (5, 6). Despite a lack of full understanding of its mechanisms of action, relaxin was tested for the treatment of systemic sclerosis. An early placebo-controlled trial showed that low-dose relaxin significantly reduced skin thickening and stabilized lung function (7). However, subsequent phase II and III trials found no significant benefit (8).

Other anti-fibrotic strategies have attempted to decrease tissue stiffness by targeting collagen cross-linking, the principal determinant of ECM stiffness. Lysyl oxidase (LOX) is an enzyme that catalyzes the covalent crosslinking of myofibroblast-secreted collagen units into insoluble fibers (9). LOX is upregulated in fibrosis and is associated with greater tissue stiffness in patients (10). Animal studies have shown that inhibition of LOX and LOX-like 2 (LOXL2) suppresses fibrosis in various organs (11, 12), however, clinical trials of LOXL2 inhibition were terminated due to lack of efficacy.

Targeting myofibroblast contractility or ECM stiffness individually has yet to be shown to be effective for the treatment of human fibrotic disease possibly because both components are linked through a positive feedback loop and likely require individualized drug-targeting. To address this possibility, we utilized the orthotopic tracheal transplant (OTT) mouse model. Rejection of OTT allografts is characterized by the destruction of the airway microvasculature and epithelial cell layer, followed by an accumulation of myofibroblasts that deposit progressively cross-linked subepithelial collagen, analogous to large airway changes seen in lung transplantation (13); OTTs do not develop bronchiolitis obliterans. Evaluating changes in OTTs permits a detailed physiologic and architectural assessment from which careful inferences can be drawn concerning the process of generalized fibrosis and fibrosis attenuation in large airways. Unlike the fibrosis in the bleomycin lung injury model which is spontaneously reversible, the fibrosis in OTTs is persistent and unresponsive to all immunomodulating agents tested to date (14) and may model certain intractable features of chronic lung allograft dysfunction (CLAD). Here, we sought to determine if

targeting both components of the biophysical microenvironment, namely myofibroblast contractility with relaxin and ECM stiffness with LOX inhibition could facilitate self-repair and reduce fibrosis after 'irreversible' tissue remodeling was well-established.

Materials and Methods

Animals and experimental procedures

Mice were acquired from the Jackson Laboratory (Bar Harbor, ME, USA.). Animal procedures were approved by the VA Palo Alto Institutional Animal Care and Utilization Committee. OTTs were performed as previously described (15). In short, tracheal segments from BALB/cJ (allograft) or C57BL/6J (syngraft) donor mice were transplanted into C57BL/6J recipient mice (wild type or B6.126-Ptger2^{tm1Brey}/J) on day 0. Twenty-one days post transplantation, mice were treated with: 1) saline; 2) recombinant human (rh) relaxin-2 at 0.5mg/kg (Novartis Pharmaceutical, Basel, Switzerland) by continuous infusion with an Alzet® mini-osmotic pump (Alzet, Cupertino, CA, USA); 3) 0.2% β-Aminopropionitrile (BAPN) (Sigma-Aldrich, St. Louis, MO, USA) in drinking water; and 4) combination of rh relaxin-2 at 0.5mg/kg and 0.2% BAPN or 5) combination of rh relaxin-2 at 0.5mg/kg with anti-LOXL2 antibody at 0.5 mg/kg (Santa Cruz Biotechnology, Dallas, TX, USA) injected daily intraperitoneally on d21-35. E prostanoid 2 (EP2) selective antagonist, PF-04418948 (Cayman Chemical, Ann Arbor, MI, USA) was injected intraperitoneally daily at 10mg/kg starting 21 days post-transplant, with or without relaxin and BAPN. Tracheas were harvested after 14 days of treatment.

Cell culture

Fibroblasts from normal (line CCL-151) (ATCC, Manassas, VA, USA) and fibrotic (line CCL-134) (ATCC; Manassas, VA, USA) human lungs were cultured in Dulbecco's Modified Eagle Medium (DMEM/F-12) (Lonza, Basel, Switzerland) supplemented with 10% fetal bovine serum, 100U/ml penicillin, and 100 ug/ml streptomycin. Fibroblasts at passage 2-5, cultured to <80 % confluency, were seeded (4647cells/cm^2) on collagen I-coated polyacrylamide gels (Matrigen, Brea, CA, USA) with elastic moduli ranging from 0.5 kPa to 25 kPa. Cells were treated with 1.2 mg/ml rh-relaxin-2 with or without PF-04418948 at 10μM in DMEM/F-12 for 20 hours after 4 hours of serum-starvation.

Immunofluorescent, Picrosirius Red, and Masson's trichrome staining

Cells were fixed with 4% paraformaldehyde, permeabilized with 0.1% Triton X-100 in phosphate-buffered saline (PBS) supplemented with 1% bovine serum albumin, and immunostained after blocking. Mouse tracheal tissues were fixed with 10% formalin, embedded in paraffin, then cut cross-sectionally with a microtome (Leica Microsystems, Wetzlar, Germany). Eight-μm tracheal cross-sections were stained by immunofluorescent, Picrosirius Red, or Masson's trichrome staining. The following primary antibodies were used: phospho-myosin light chain (pMLC) mAb (Cell Signaling Technology, Danvers, MA, USA), pro-collagen type I mAb, cyclooxygenase-2 (COX-2) mAb, leucine-rich repeat–containing G protein-coupled receptor 7 (LGR7/ RXFP1) pAb (from Abcam, Cambridge, MA, USA), and conjugated (Cy®3) α-SMA mAb (Sigma-Aldrich, St. Louis, MO, USA) at a 1:200 dilution. For *in vitro* experiments, collagen production was assessed by expression of

procollagen I (ProColI), a precursor of collagen; fibroblast to myofibroblast differentiation was assessed by α-SMA expression. The contraction of myofibroblasts was evaluated and measured by immunofluorescent staining of pMLC and traction force microscopy. Expressions of relaxin receptor on myofibroblasts were evaluated by immunofluorescent staining of RXFP1. Corrected total cell fluorescence was measured by Image J, and was defined as CTCF = Integrated Density of Selected Cell − (Area of Selected Cell × Mean Fluorescence of Back Ground Readings). Anti-rabbit Alexa Fluor® 488m, anti-rabbit Cy®3, and anti-rat Cy®3 were used for secondary antibodies (Invitrogen, Carlsbad, CA, USA).

Hydroxyproline assay

Mice tracheas were weighed, homogenized, and hydrolyzed in hydrochloric acid (12N). Hydroxyproline concentrations were measured according to the manufacturer's instructions (BioVision, Milpitas, CA, USA).

Immunosorbent assays and immunoblot analysis

For immunosorbent assays, supernatants were collected and PGE_2 concentrations were detected by enzyme-linked immunosorbent assay (ELISA) according to the manufacturer's instructions (Cayman Chemical, Ann Arbor, MI, USA). For immunoblot analysis, cells were rinsed with PBS and lysed with radio-immunoprecipitation assay buffer supplemented with Halt® protease and phosphatase inhibitor cocktail, stabilized in dimethylsulfoxide (Thermo Fisher Scientific, Waltham, MA, USA). Cell lysates were loaded onto SDS-polyacrylamide gels followed by electrophoresis and immunoblot analysis using chemiluminescent immunodetection.

Traction Force Microscopy

Traction generated by individual cells was measured as described previously (16). Cells were plated at 2 cells/mm^2 on collagen-coated polyacrylamide gels, embedded with fluorescent beads (0.5 μm). Twenty-four hours later, a phase contrast image and an image of the fluorescent beads immediately underneath the cell were taken. The cells were detached from the gels and a second image of the same fluorescent beads was taken. Displacement maps and traction fields were obtained by cross-correlating these images.

Statistical analysis

Sharpiro-Wilk test was performed to test if the data were normally distributed. Statistical significance ($P<0.05$) was assessed using the unpaired t-test assuming unequal variances between the treatment and saline-control groups for hydroxyproline analysis (Prism Software, Irvine, CA, USA). In Figure 5, where multiple group comparisons are made, a one-way ANOVA test was used. For histologic analysis, at least 10 tissue sections from each animal (3-20 animals per group) were examined and analyzed with the Mann-Whitney test. Analysis of collagen density in trichrome stained sections was measured by the ratio of the blue area to the area between the subepithelium and cartilage with Image J. For *in vitro* studies, results are from at least 3 independent experiments, and the statistical significance ($P<0.05$) was assessed using the Mann-Whitney test.

Results

Combined treatment with relaxin and LOX inhibition attenuates established airway fibrosis

Previous studies showed that monotherapy with relaxin or LOX inhibition is effective in preventing fibrosis in animal models (7, 8). We asked whether these drugs could reverse the airway fibrosis in OTT recipients. Non-immunosuppressed allograft OTT mice were treated at 21 days post transplantation, a time point at which fibrosis is well-established (Figure S1). These mice were treated with relaxin, BAPN, LOXL2, relaxin with BAPN, relaxin with LOXL2, or saline for 14 days (Figure 1A). Relaxin monotherapy minimally decreased subepithelial collagen deposition while BAPN monotherapy had no effect. However, combined relaxin and BAPN treatment significantly diminished collagen deposition in the subepithelial layer as demonstrated by histology and hydroxyproline concentration (Figure 1B-D). Moreover, combined treatment with relaxin and BAPN promoted tracheal re-epithelialization with taller cuboidal and pseudostratified epithelium, compared to animals in other groups, which exhibited flattened epithelium (Figure 1B, E). Substitution of BAPN with less toxic LOXL2 antibody in combined therapy modestly decreased subepithelial collagen. There was a trend toward decreased hydroxyproline concentration, but this did not meet statistical significance (Figure S2, *P*=0.0542).

Decrease in cellular contractility with relaxin is dependent on the type of fibroblast and matrix stiffness

The *in vivo* data indicated that relaxin in combination with LOX inhibition significantly decreased collagen deposition, which suggests the effectiveness of relaxin may be ECM-stiffness-dependent. Prior studies have isolated the role of matrix stiffness in cellular functions by plating cells on inert cross-linked polyacrylamide hydrogels (17). The effect of LOX inhibition in our study was modeled *in vitro* by varying the stiffnesses of these matrices. This was used as a surrogate for BAPN because the use of polyacrylamide gels allow one to isolate the contribution of matrix stiffness whereas a collagen matrix is limited by the fact that plated cells can migrate into the matrix, changing the stiffness. Also, it should be noted that since BAPN inhibits collagen crosslinking, it has no action on a polyacrylamide gel.

One measure of stiffness is Young's elastic modulus, which is defined as the force per unit area (Pascal (Pa)) required to deform a given material. Shkumatov *et al.* measured the stiffness of intrapulmonary airways in the mouse lung by atomic force microscopy and found that the elastic moduli range from 2-45 kPa, with median of 18.6 kPa (18). In another study, Booth *et al.* found that the mean Young's modulus of normal human lungs was 2 kPa while that of tissue from idiopathic pulmonary fibrotic lungs was 16 kPa (19). Therefore, we used 0.5 kPa and 4 kPa matrices to mimic low lung tissue stiffness and 12 kPa and 25 kPa matrices to mimic intermediate to high lung tissue stiffness.

On soft matrices (0.5 kPa, 4kPa), there was no detectable expression of ProColI, α-SMA, or pMLC in normal lung fibroblasts (Figure S3, Figure 2A). On stiff matrices (12 kPa, 25 kPa), the expressions of ProColI (Figure S3), α-SMA and pMLC (Figure 2A) were all significantly increased. Relaxin inhibited expression of these markers in normal lung

fibroblasts plated on intermediate stiffness (12 kPa) but not in cells plated on the highest stiffness matrices (25 kPa) (Figure 2A).

Lung fibroblasts from 'stiff' conditions (i.e. fibrotic lung) have been shown to be more contractile than those from normal lungs (20). Therefore, we questioned whether relaxin would regulate the contraction of fibrotic lung fibroblasts and normal lung fibroblasts differently. We found fibrotic lung fibroblasts were more contractile even on a relatively low matrix stiffness of 4 kPa (Figure 2B). At 4 kPa, relaxin was able to decrease the expression of pMLC (Figure 2B). However, on matrices with intermediate and high stiffnesses, relaxin failed to reduce pMLC expressions. Immunoblots showed that in normal lung fibroblasts, treatment with relaxin significantly decreased pMLC expression at 12 kPa (Figure 2C), but in fibrotic lung fibroblasts, relaxin decreased pMLC expression only at 4 kPa (Figure 2D).

To further examine relaxin's effects on cell contraction, we quantified the contractility of fibrotic and normal lung fibroblasts by traction force microscopy (16). We found both normal and fibrotic lung fibroblasts exhibited increased contractions with increasing substrate stiffness as measured by root mean square tractions (RMST) (Figure 3). Treatment with relaxin decreased the contraction of normal lung fibroblasts plated on 12 kPa matrices but had no significant effects on cells plated on matrices with higher stiffness (Figure 3A, C). Treatment with relaxin decreased the contraction of fibrotic lung fibroblasts plated on 4kPa matrices but had no effects on cells plated on matrices with elastic moduli of 12 KPa and higher (Figure 3B, D).

Expression of relaxin receptor 1 (RXFP1) on fibroblasts is modulated in response to increases in matrix stiffness

Tan *et al.* found that RXFP1 is significantly decreased in the lungs of idiopathic pulmonary fibrosis (IPF) patients, and suggested that progression of IPF may be associated with sequential decreases of RXFP1 expression (21). In our study, because relaxin's positive effects were dampened by a stiff microenvironment *in vitro*, we speculated that the expression of RXFP1 is modulated by a progressive increase in ECM stiffness. We found expression levels of RXFP1 were significantly higher on fibroblasts plated on soft matrices (0.5 kPa and 4kPa) than those on fibroblasts cultured on intermediate and stiff matrices (12 kPa and 25 kPa) (Figure 4A,C). Interestingly, cells that expressed higher levels of α-SMA had lower RXFP1 expressions (Figure 4A) than expressing lower or non-detectable levels of α-SMA. Fibrotic lung fibroblasts had much lower expressions of RXFP1 than normal lung fibroblasts. Expression levels of RXFP1 were significant decreased on fibrotic lung fibroblasts plated on matrices with elastic moduli of 4 kPa and higher (Figure 4 B, D).

Combined relaxin and LOX inhibition efficacy is COX-2/PGE$_2$-dependent

Next, to address how relaxin may augment LOX inhibition, we evaluated a key eicosanoid implicated in lung fibrosis regulation, PGE$_2$. PGE$_2$ is generated when COX-2 catalyzes the oxidation of arachidonic acid, and is the predominant prostaglandin in the lung (22, 23, 24). PGE$_2$ has been shown to decrease cell contractility, and levels of COX-2/PGE$_2$ are significantly decreased in lung fibroblasts (22, 25). This led us to investigate whether the

effectiveness of combined relaxin and BAPN therapy was mediated through the COX-2/PGE$_2$ pathway.

Mouse tracheal allografts of saline control, relaxin monotherapy, and BAPN monotherapy groups had negligible levels of COX-2 expression (Figure 5A). By distinction, tracheas from mice treated with both relaxin and BAPN demonstrated levels of COX-2 expression in the epithelium and subepithelium similar to that of tissue from syngrafts. Next, we assessed the expression of COX-2 in normal lung fibroblasts on substrates with elastic moduli ranging from 0.5 kPa-25 kPa. Cells plated on stiff matrices had less COX-2 expression than those plated on soft matrices, verifying previous observations (1). Relaxin increased COX-2 content in cells from 0.5 and 4 kPa matrices but not from the 12 or 25 kPa matrices (Figure 5B). Supernatants of fibroblasts plated on matrices of physiologic stiffness (0.5, 1, and 2 kPa) had higher concentrations of PGE$_2$ than those of cells plated on stiffer matrices (4, 12, and 25 kPa). Relaxin increased PGE$_2$ levels on all but the stiffest matrices (25 kPa) (Figure 5C).

PGE$_2$ can ligate four distinct G protein-coupled receptors, termed EP receptors 1-4. Numerous reports have implicated EP$_2$ as the major receptor mediating inhibitory effects on indices of fibroblast activation (26, 27). To confirm that relaxin mediates a decrease in cell contraction by upregulating COX-2/PGE$_2$ production and signaling via the EP$_2$ receptor, we inhibited the actions of PGE$_2$ by treating normal lung fibroblasts with PF-04418948, a potent and selective EP$_2$ antagonist. This EP$_2$ antagonist prevented the relaxin-mediated reduction of pMLC and α-SMA in cells cultured on the 12 kPa matrices (Figure 6A).

To test whether the beneficial effects of the combined treatment of relaxin and BAPN *in vivo* could be abrogated by inhibition of the COX-2/PGE$_2$/EP$_2$ pathway, OTT mice, 21 days post transplantation, were treated with saline, PF-04418948, or combined relaxin and BAPN treatment with or without PF-04418948. Furthermore, OTT EP$_2$ receptor knock-out (EP$_2$ KO) mice (B6.126-Ptger2^{tm1Brey}/J) were treated with or without the combination of relaxin and BAPN. Suppression of PGE$_2$ signaling with the EP$_2$ receptor antagonist in the combined treatment group abrogated the protective effect of combined treatment, with specimens exhibiting dense deposition of subepithelial collagen and no restoration of cuboidal epithelium (Figure 6B, C). Similarly, treatment with relaxin and BAPN lost its beneficial effects in EP$_2$ KO mice. Tracheas from PF-04418948 treated mice and EP$_2$ KO mice had higher amounts of collagen than those from saline treated control mice as shown in hydroxyproline concentration measurement. Combined treatment of relaxin and BAPN failed to decrease collagen amount in tracheas from PF-04418948 treated wild type and EP$_2$ KO mice (Figure 6C, D), providing further support that relaxin and BAPN act through the COX-2/PGE$_2$/EP$_2$ pathway.

Discussion

Pre-clinical studies have used a large number of therapies that have demonstrated the reversal of fibrosis in animal models. However, very few of these have been found to be effective in human fibrotic diseases. The discrepancy between the pre-clinical and clinical findings may, in part, be due to the use of models of fibrosis that are not robust. Compared to

other fibrotic models, such as the bleomycin-injured lung model which is spontaneously reversible, the tissue remodeling in the OTT model is particularly robust and progressive, driven by inflammation (alloimmunity) not present in non-transplant models of fibrosis. Treatment of the OTT model with numerous immunosuppressant and anti-fibrotic agents, including high dose steroids, anti-CD40L, anti-Lymphocyte function-associated antigen 1 (anti-LFA-1), combined anti-CD40L / anti-LFA-1 (14), and Pirfenidone, have not been able to reverse fibrosis (additional data not shown). In this study, we demonstrated that combined therapy with relaxin and LOX inhibition reversed established airway fibrosis by targeting both intracellular and extracellular biophysical properties of the graft -cellular contractility and ECM stiffness-, and in this manner, appeared to promote the conversion towards a normal, non-remodeled, epithelialized airway.

As described above, myofibroblast activation and contraction contribute to ECM stiffening and further fibrotic progression. Myofibroblast contractility is regulated by MLC phosphorylation, which enables myosin to interact with actin filaments to generate force. We found that pMLC and root mean square traction of lung fibroblasts cultured on soft and intermediate stiff matrices were down-regulated by relaxin. Relaxin also decreased α-SMA and ProcolI expression in normal lung fibroblasts on matrices of soft/intermediate stiffness but lost its effects on very stiff matrices. In the mouse OTT model, monotherapy with relaxin had only a minimal effect in reversing fibrosis. Given the *in vitro* findings, we suspect that relaxin alone was not effective in reversing fibrosis in OTT model (and possible fibrosis in human) because the ECM of the tracheas was already very stiff.

Relaxin was first named for its ability to relax the female reproductive tract during pregnancy (28). It is produced in both genders and has been shown to act intracellularly to induce cellular relaxation and ameliorate fibrosis (29). Relaxin and its G-protein coupled receptors are found in rodent and human lungs, predominantly within bronchial epithelial cells, fibroblasts, and airway smooth muscle cells (6, 30). Intriguingly, relaxin-deficient mice develop age-associated fibrosis in the lung and skin (31, 32). However, as stated above, phase 2 and 3 trials of relaxin did not demonstrate any efficacy in the treatment of fibrosis in systemic sclerosis (8). It has been shown that RXFP1 level is decreased in lungs of IPF patients (21). We found that fibroblasts that were plated on stiff matrices had significant lower RXFP1 expressions than those plated on soft matrices. This may suggest that expression of RXFP1 is associated with progressive increase of ECM stiffness in fibrosis. Therefore, we speculate that the lack of an effect in established dermal fibrosis may have been due to the relatively high tissue stiffness.

Tissue stiffening mainly results from the cross-linking of ECM proteins (33). LOX converts collagen from soluble monomers to insoluble fibers by oxidizing peptidyl lysine to form covalent cross-linkages, thereby increasing ECM stiffness (9). Inhibition of LOX with BAPN decreased α-SMA expression and fibrotic tissue stiffness in a carbon tetrachloride-induced liver fibrosis model. (11). In a bleomycin lung model, inhibition of LOXL2 with a monoclonal antibody decreased collagen deposition (12). Nevertheless, clinical phase 2 trial was terminated due to lack of efficacy. Intriguingly, current study models persistent alloimmune injury, LOX inhibitor monotherapy failed to reverse established fibrosis. We modeled the effect of LOX inhibition and isolated the role of substrate stiffness by plating

cells on inert polyacrylamide gels with stiffnesses ranging from normal to fibrotic tissues. We found that soft (0.5, 4 kPa) but not intermediate or stiff substrates (12, 25 kPa), prevented expression of ProColI and the differentiation and contraction of fibroblasts. These findings suggest that the stiffness of chronically-rejected trachea is stiffer than normal airways (range from 2-45 kPa in previous study), and exceeded the threshold below which the profibrotic feedback loop could be interrupted by LOX inhibition alone.

Fibrotic lungs express less $COX-2/PGE_2$ than healthy lungs (34). We found that allogeneic transplanted tracheas have less COX-2 and more α-SMA expression than syngeneic transplants. Allografts from mice treated with combined relaxin/LOX inhibition express more COX-2 than those from monotherapies. *In vitro*, relaxin up-regulated COX-2 expression and PGE_2 secretion in fibroblasts cultured on soft matrices but not on stiff matrices. Relaxin boosted the secretion of endogenous PGE_2 from cells on low to intermediate stiffness matrices, but failed to increase PGE_2 levels in cells cultured on pathological stiff matrices (25 kPa). These results suggest that relaxin's ability to upregulate $COX-2/PGE_2$ is dampened by a stiff microenvironment. This was also observed in previous studies that demonstrate that a stiff ECM suppresses the secretion of $COX-2/PGE_2$. Previous investigations showed PGE_2 signaling through the EP_2 receptor inhibits lung myofibroblast differentiation, contraction, and secretion of collagen (26, 35). We found that treatment with an EP_2 receptor antagonist abrogated the effects of relaxin on cells cultured in the intermediate stiff matrices as well as the beneficial effects of combined treatment on fibrotic airways. These results cumulatively indicate that the effectiveness of combined relaxin and BAPN treatment in abrogating subepithelial fibrosis is mediated through COX-2 expression, PGE_2 biosynthesis, and EP_2 signaling.

In addition to decreasing myofibroblast contractility directly, PGE_2 has also been shown to inhibit LOX (36), which may contribute to further decreasing collagen cross-linking and softening of the ECM. Moreover, Liu *et al.* demonstrated that a stiff ECM suppresses the $COX-2/PGE_2$ pathway (1). Thus, decreasing collagen cross-linking with LOX inhibition, itself, may lead to increased $COX-2/PGE_2$, which in turn, can decrease myofibroblast contractility. These mechanisms may further support the reversal of fibrosis (Figure 6E).

Combined treatment not only decreased subepithelial fibrosis, but also promoted an epithelium expressing high level of COX-2. Konoeda *et al.* showed that fibrosis in the chronically-rejected airways is associated with an aberrant flattened epithelium, and the damage to epithelial cells appears before the subepithelial fibrosis (37). In contrast to the flattened epithelium observed in other treatment groups, mice treated with combined therapy had taller, more cuboidal, and occasionally pseudostratified, epithelial layers. Because the airway epithelium is a major source of PGE_2 (38), its damage could lead to decreased levels of PGE_2 in the airway and an inability to inhibit fibroblast proliferation and activation, thereby promoting subepithelial fibrosis. However, the mechanism by which combined therapy with relaxin and LOX inhibition contributed to the development of this columnar epithelium requires further investigation. Prior studies showed PGE_2 deficiency in lung fibrosis leads to increased airway epithelial cell apoptosis and PGE_2 has been shown to promote epithelial cell proliferation and migration (39, 40). We speculate that the collagen-

rich subepithelium is unable to support a pseudostratified columnar epithelium perhaps, in part, due to a deficiency of COX-2/PGE$_2$.

One limitation of this study is that we were unable to confirm that LOX inhibition decreased tracheal stiffness, in vivo. We attempted to measure the elastic moduli of the tracheas with AFM, but found that there was wide variability within each sample with point to point differences up to 10 kPas (data not shown). Previous studies have shown that the Young's elastic moduli of non-cartilaginous lung airways range from 2-45 kPa (18). We suspect that the variability in cartilaginous airways will be even higher. Another limitation of this study is that although BAPN is a potent irreversible inhibitor of LOX, wider clinical use is limited by its side effects, such as osteolethyrism, a disorder that can lead to skeletal deformations (41). We replaced BAPN with nontoxic LOXL2 antibody and found the combined treatment of relaxin and LOXL2 had a less significant effect on reduction of collagen. BAPN was used in this study as a proof of concept; for clinical use, other less toxic and more potent LOX or LOX-like inhibitors in conjunction with relaxin could be tested.

In summary, we demonstrated reversal of transplanted airway fibrosis by targeting both intracellular and extracellular biophysical properties of the allograft. We show that relaxin increases the expression of COX-2/PGE$_2$, thus decreasing cellular contraction while LOX inhibition presumptively decreases tissue stiffness and together may shift the airway toward a physiologic state (Figure 6E). The reversal of established fibrosis achieved in this work may represent a novel therapeutic strategy for the treatment of chronic rejection in solid organ transplantation as well as other fibrotic diseases.

Supplementary Material

Refer to Web version on PubMed Central for supplementary material.

Acknowledgments

Abbreviations

α-SMA	α-smooth muscle actin
BAPN	β-Aminopropionitrile
COX-2	cyclooxygenase-2
ECM	extracellular matrix
EP-2	E prostanoid 2
LOX	lysyl oxidase
LOXL-2	lysyl oxidase like 2

OTT	orthotopic tracheal transplantation
PGE$_2$	prostaglandin E-2
pMLC	phospho-myosin light chain
ProcolI	pro-collagen type I
RMST	root mean square tractions

References

1. Liu F, Mih JD, Shea BS, Kho AT, Sharif AS, Tager AM, et al. Feedback amplification of fibrosis through matrix stiffening and COX-2 suppression. Journal of Cell Biology. 2010; 190(4):693–706. [PubMed: 20733059]

2. Klingberg F, Hinz B, White ES. The myofibroblast matrix: implications for tissue repair and fibrosis. Journal of Pathology. 2013; 229(2):298–309. [PubMed: 22996908]

3. Wipff P-J, Rifkin DB, Meister J-J, Hinz B. Myofibroblast contraction activates latent TGF-beta 1 from the extracellular matrix. Journal of Cell Biology. 2007; 179(6):1311–1323. [PubMed: 18086923]

4. Zhou Y, Huang XW, Hecker L, Kurundkar D, Kurundkar A, Liu H, et al. Inhibition of mechanosensitive signaling in myofibroblasts ameliorates experimental pulmonary fibrosis. J Clin Invest. 2013; 123(3):1096–1108. [PubMed: 23434591]

5. Huang X, Gai Y, Yang N, Lu B, Samuel CS, Thannickal VJ, et al. Relaxin Regulates Myofibroblast Contractility and Protects against Lung Fibrosis. American Journal of Pathology. 2011; 179(6): 2751–2765. [PubMed: 21983071]

6. Royce SG, Miao YR, Lee M, Samuel CS, Tregear GW, Tang MLK. Relaxin Reverses Airway Remodeling and Airway Dysfunction in Allergic Airways Disease. Endocrinology. 2009; 150(6): 2692–2699. [PubMed: 19213838]

7. Seibold JR, Korn JH, Simms R, Clements PJ, Moreland LW, Mayes MD, et al. Recombinant human relaxin in the treatment of scleroderma - A randomized, double-blind, placebo-controlled trial. Annals of Internal Medicine. 2000; 132(11):871–879. [PubMed: 10836913]

8. Seibold JR. Relaxins: lessons and limitations. Current rheumatology reports. 2002; 4(4):275–276. [PubMed: 12126574]

9. Lucero HA, Kagan HM. Lysyl oxidase: an oxidative enzyme and effector of cell function. Cellular and Molecular Life Sciences. 2006; 63(19-20):2304–2316. [PubMed: 16909208]

10. Lopez B, Gonzalez A, Hermida N, Valencia F, de Teresa E, Diez J. Role of lysyl oxidase in myocardial fibrosis: from basic science to clinical aspects. American Journal of Physiology-Heart and Circulatory Physiology. 2010; 299(1):H1–H9. [PubMed: 20472764]

11. Georges PC, Hui J-J, Gombos Z, McCormick ME, Wang AY, Uemura M, et al. Increased stiffness of the rat liver precedes matrix deposition: implications for fibrosis. American Journal of Physiology-Gastrointestinal and Liver Physiology. 2007; 293(6):G1147–G1154. [PubMed: 17932231]

12. Barry-Hamilton V, Spangler R, Marshall D, McCauley S, Rodriguez HM, Oyasu M, et al. Allosteric inhibition of lysyl oxidase-like-2 impedes the development of a pathologic microenvironment. Nature Medicine. 2010; 16(9):1009–U1107.

13. Genden EM, Boros P, Liu JH, Bromberg JS, Mayer L. Orthotopic tracheal transplantation in the murine model. Transplantation. 2002; 73(9):1420–1425. [PubMed: 12023619]

14. Babu AN, Murakawa T, Thurman JM, Miller EJ, Henson PM, Zamora MR, et al. Microvascular destruction identifies murine allografts that cannot be rescued from airway fibrosis. Journal of Clinical Investigation. 2007; 117(12):3774–3785. [PubMed: 18060031]

15. Jiang X, Khan MA, Tian W, Beilke J, Natarajan R, Kosek J, et al. Adenovirus-mediated HIF-1 alpha gene transfer promotes repair of mouse airway allograft microvasculature and attenuates chronic rejection. Journal of Clinical Investigation. 2011; 121(6):2336–2349. [PubMed: 21606594]

16. Butler JP, Tolic-Norrelykke IM, Fabry B, Fredberg JJ. Traction fields, moments, and strain energy that cells exert on their surroundings. American Journal of Physiology-Cell Physiology. 2002; 282(3):C595–C605. [PubMed: 11832345]

17. Pelham RJ, Wang YL. Cell locomotion and focal adhesions are regulated by substrate flexibility. Proceedings of the National Academy of Sciences of the United States of America. 1997; 94(25): 13661–13665. [PubMed: 9391082]

18. Shkumatov A, Thompson M, Choi KM, Sicard D, Baek K, Kim DH, et al. Matrix stiffness-modulated proliferation and secretory function of the airway smooth muscle cells. American Journal of Physiology-Lung Cellular and Molecular Physiology. 2015; 308(11):L1125–L1135. [PubMed: 25724668]

19. Booth AJ, Hadley R, Cornett AM, Dreffs AA, Matthes SA, Tsui JL, et al. Acellular Normal and Fibrotic Human Lung Matrices as a Culture System for In Vitro Investigation. American Journal of Respiratory and Critical Care Medicine. 2012; 186(9):866–876. [PubMed: 22936357]

20. Hinz B. Mechanical aspects of lung fibrosis: a spotlight on the myofibroblast. Proceedings of the American Thoracic Society. 2012; 9(3):137–147. [PubMed: 22802288]

21. Tan J, Tedrow JR, Dutta JA, Juan-Guardela B, Nouraie M, Chu Y, et al. Expression of RXFP1 is Decreased in Idiopathic Pulmonary Fibrosis: Implications for Relaxin-Based Therapies. American journal of respiratory and critical care medicine. 2016 DOI: 10.1164/rccm.201509-1865OC.

22. Wilborn J, Crofford LJ, Burdick MD, Kunkel SL, Strieter RM, Petersgolden M. Cultured Lung Fibroblasts Isolated from Patients with Idiopathic Pulmonary Fibrosis Have a Diminished Capacity to Synthesize Prostaglandin E(2), and to Express Cyclooxygenase-2. Journal of Clinical Investigation. 1995; 95(4):1861–1868. [PubMed: 7706493]

23. Huang SK, Peters-Golden M. Eicosanoid lipid mediators in fibrotic lung diseases: Ready for prime time? Chest. 2008; 133(6):1442–1450. [PubMed: 18574287]

24. Ozaki T, Rennard SI, Crystal RG. Cyclooxygenase Metabolites are Compartmentalized in the Human Lower Respiratory-tract. Journal of Applied Physiology. 1987; 62(1):219–222. [PubMed: 3104286]

25. Borok Z, Gillissen A, Buhl R, Hoyt RF, Hubbard RC, Ozaki T, et al. Augmentation of Functional Prostaglandin-E Levels on the Respiratory Epithelial Surface by Aerosol Administration of Prostaglandin-E. American Review of Respiratory Disease. 1991; 144(5):1080–1084. [PubMed: 1952435]

26. Kolodsick JE, Peters-Golden M, Larios J, Toews GB, Thannickal VJ, Moore BB. Prostaglandin E-2 inhibits fibroblast to myofibroblast transition via E. prostanoid receptor 2 signaling and cyclic adenosine monophosphate elevation. American Journal of Respiratory Cell and Molecular Biology. 2003; 29(5):537–544. [PubMed: 12738687]

27. Huang S, Wettlaufer SH, Hogaboam C, Aronoff DM, Peters-Golden M. Prostaglandin E-2 inhibits collagen expression and proliferation in patient-derived normal lung fibroblasts via E prostanoid 2 receptor and cAMP signaling. American Journal of Physiology-Lung Cellular and Molecular Physiology. 2007; 292(2):L405–L413. [PubMed: 17028262]

28. Hisaw FL. Experimental relaxation of the pubic ligament of the guinea pig. Proceedings of the Society for Experimental Biology and Medicine. 1926; 23(8):661–663.

29. Bennett RG. Relaxin and its role in the development and treatment of fibrosis. Translational Research. 2009; 154(1):1–6. [PubMed: 19524867]

30. Hsu SY, Nakabayashi K, Nishi S, Kumagai J, Kudo M, Sherwood OD, et al. Activation of orphan receptors by the hormone relaxin. Science. 2002; 295(5555):671–674. [PubMed: 11809971]

31. Samuel CS, Zhao C, Bathgate RAD, Bond CP, Burton MD, Parry LJ, et al. Relaxin deficiency in mice is associated with an age-related progression of pulmonary fibrosis. FASEB Journal. 2003; 17(1):121–123. [PubMed: 12424226]

32. Samuel CS, Royce SG, Chen B, Cao H, Gossen JA, Tregear GW, et al. Relaxin Family Peptide Receptor-1 Protects against Airway Fibrosis during Homeostasis But Not against Fibrosis Associated with Chronic Allergic Airways Disease. Endocrinology. 2009; 150(3):1495–1502. [PubMed: 18974264]

33. Parker MW, Rossi D, Peterson M, Smith K, Sikstrom K, White ES, et al. Fibrotic extracellular matrix activates a profibrotic positive feedback loop. Journal of Clinical Investigation. 2014; 124(4):1622–1635. [PubMed: 24590289]

34. Huang SK, White ES, Wettlaufer SH, Grifka H, Hogaboam CM, Thannickal VJ, et al. Prostaglandin E-2 induces fibroblast apoptosis by modulating multiple survival pathways. Faseb Journal. 2009; 23(12):4317–4326. [PubMed: 19671668]

35. Garrison G, Huang SK, Okunishi K, Scott JP, Penke LRK, Scruggs AM, et al. Reversal of Myofibroblast Differentiation by Prostaglandin E-2. American Journal of Respiratory Cell and Molecular Biology. 2013; 48(5):550–558. [PubMed: 23470625]

36. Boak AM, Roy R, Berk J, Taylor L, Polgar P, Goldstein RH, et al. Regulation of Lysyl Oxidase Expression in Lung Fibroblasts by Transforming Growth Factor-beta(1) and Prostaglandin E(2). American Journal of Respiratory Cell and Molecular Biology. 1994; 11(6):751–755. [PubMed: 7946403]

37. Konoeda C, Koinuma D, Morishita Y, Sano A, Nagayama K, Motomura N, et al. Epithelial to Mesenchymal Transition in Murine Tracheal Allotransplantation: An Immunohistochemical Observation. Transplant Proc. 2013; 45(5):1797–1801. [PubMed: 23769046]

38. Lama V, Moore BB, Christensen P, Toews GB, Peters-Golden M. Prostaglandin E-2 synthesis and suppression of fibroblast proliferation by alveolar epithelial cells is cyclooxygenase-2-dependent. American Journal of Respiratory Cell and Molecular Biology. 2002; 27(6):752–758. [PubMed: 12444036]

39. Maher TM, Evans IC, Bottoms SE, Mercer PF, Thorley AJ, Nicholson AG, et al. Diminished Prostaglandin E-2 Contributes to the Apoptosis Paradox in Idiopathic Pulmonary Fibrosis. American Journal of Respiratory and Critical Care Medicine. 2010; 182(1):73–82. [PubMed: 20203246]

40. Savla U, Appel HJ, Sporn PHS, Waters CM. Prostaglandin E-2 regulates wound closure in airway epithelium. American Journal of Physiology-Lung Cellular and Molecular Physiology. 2001; 280(3):L421–L431. [PubMed: 11159024]

41. Dawson DA, Rinaldi AC, Poch G. Biochemical and toxicological evaluation of agent-cofactor reactivity as a mechanism of action for osteolathyrism. Toxicology. 2002; 177(2-3):267–284. [PubMed: 12135629]
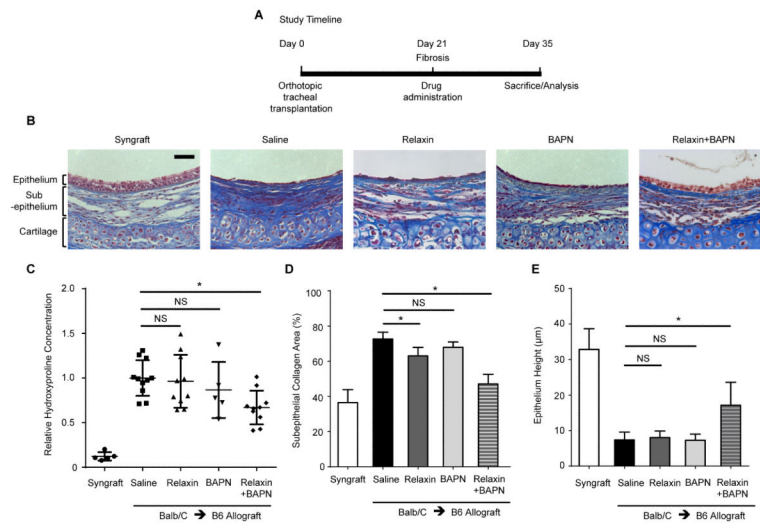
Figure 1.

Combined treatment with relaxin and LOX inhibition attenuates established fibrosis in the OTT model. Tracheal segments from donor mice were transplanted orthotopically into major histocompatibility complex (MHC)-matched (syngraft) or mismatched (allograft) recipient mice on day 0. (A) Non-immunosuppressed OTT mice were subjected to treatment at day 21, when fibrosis is well-established, for 14 days. Mice were treated with recombinant human relaxin-2 or saline, with or without the LOX inhibitor, 0.2% β-Aminopropionitrile (BAPN). (B) Representative images of Masson trichrome staining of tracheal cross-sections, in which collagen was stained in blue. Scale bar = 50 μm. (C) Hydroxyproline concentration in tracheal hydrolysates relative to controls was measured to assess the amount of collagen; Mean ± SD. (D) Analysis of collagen density in trichrome stained sections measured by the ratio of the blue area to the area between the subepithelium and cartilage with Image J; Mean ± SEM. (E) Measurement of epithelial thickness in tracheal cross-sections from different groups; Mean ± SEM. $*P < 0.05$. For B, D, E, n=3-10 per group with at least 10 tissue sections per animal.
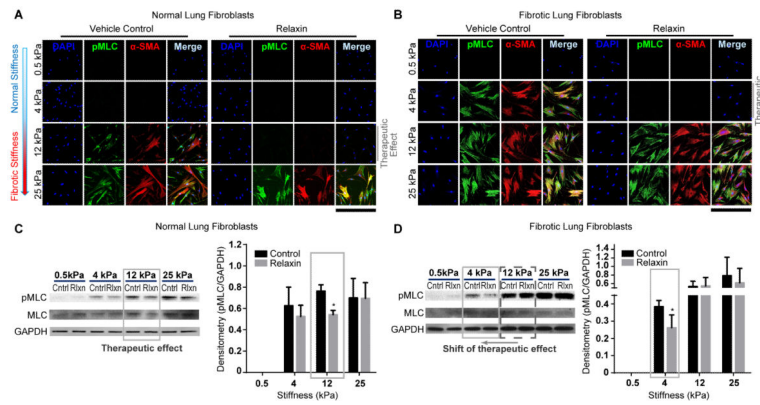
Figure 2.
Decrease in cellular contractility with relaxin is dependent on the type of fibroblast and matrix stiffness. Immunofluorescent staining and immunoblot analysis of normal and fibrotic lung fibroblasts. All results are from at least 3 independent experiments. (A, B) Immunofluorescent staining of normal (A) and fibrotic (B) lung fibroblasts cultured on matrices with Young's elastic moduli of 0.5-25 kilopascal (kPa) with and without relaxin. The contraction of cells was evaluated by expression of phospho-myosin light chain (pMLC). Fibroblast to myofibroblast differentiation was assessed by α-smooth muscle actin (α-SMA) expression; Scale bar =424 μm. (C, D) Immunoblot analysis of normal (C) and fibrotic (D) lung fibroblasts cultured on matrices with different elastic moduli. Cells were treated without (Cntrl) or with relaxin (Rlxn). The graph represents quantification of the immunoblots by densitometry. Mean ± SEM. *P<0.05.
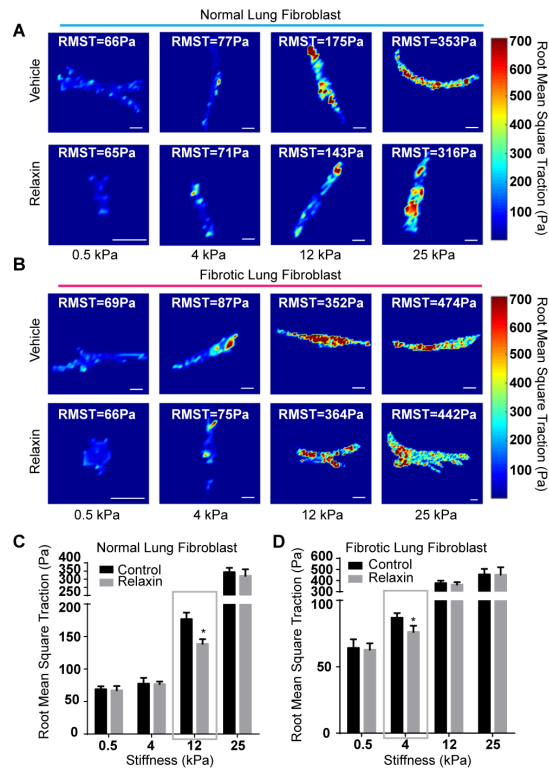
Figure 3.
Root mean square tractions (RMST) of cells measured by traction force microscopy. (A, B) Representative traction fields in Pascals (Pa) of normal (A) and fibrotic (B) lung fibroblasts plated on matrices with Young's elastic moduli 0.5-25 kPa. (C, D) Analysis of RMST of normal (C) and fibrotic (D) lung fibroblasts plated on matrices with different elastic moduli. Mean ± SEM. n=8-15 per group, scale bars=20 μm, *P<0.05.
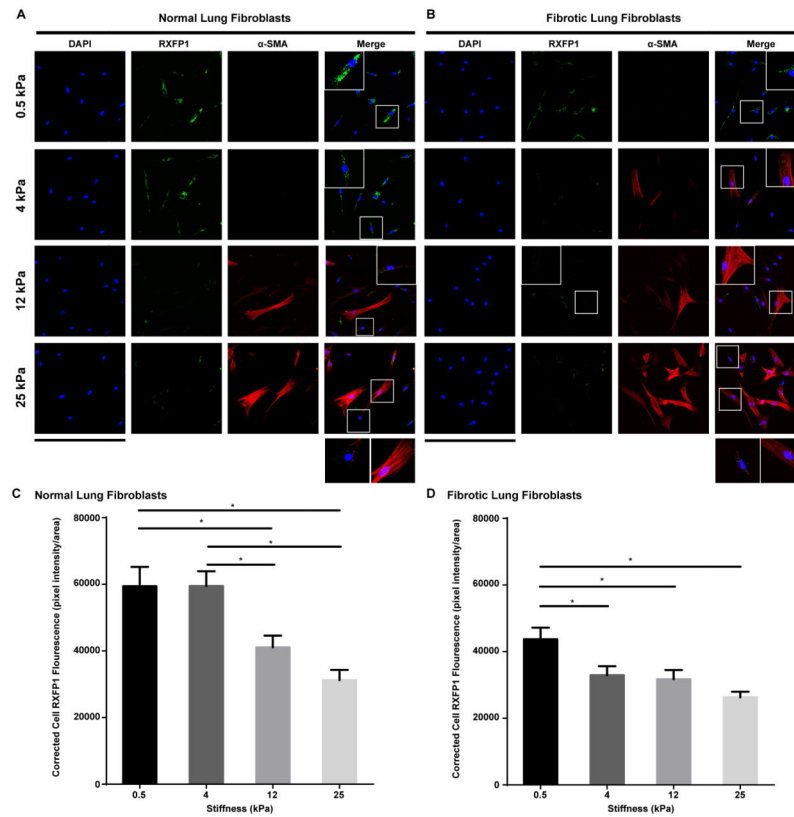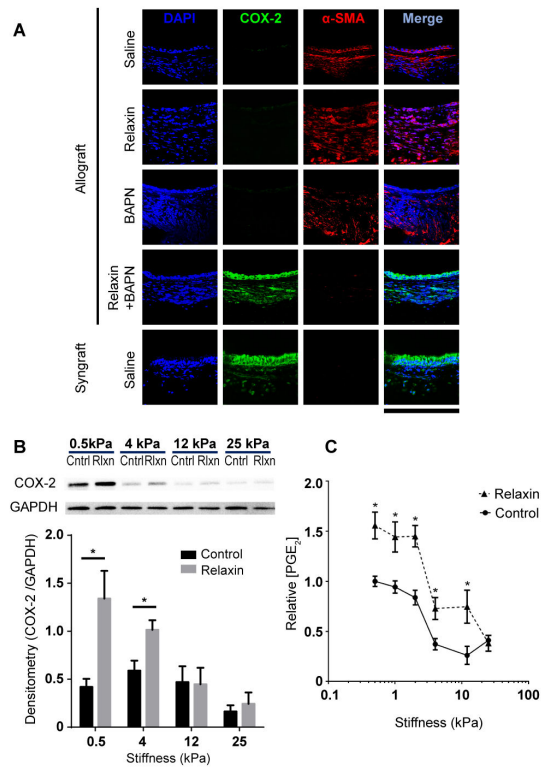
Figure 4.
Expression of relaxin receptor 1 (RXFP1) on fibroblasts. (A, B) Immunofluorescent staining of RXFP1 on normal (A) and fibrotic (B) lung fibroblasts cultured on matrices with Young's elastic moduli of 0.5-25 kilopascal (kPa). Fibroblast to myofibroblast differentiation was assessed by α-smooth muscle actin (α-SMA) expression; scale bar =424 μm; inserts are 4X magnification of selected area. (C, D) Corrected total cell fluorescence of normal (C) and fibrotic (D) lung fibroblasts cultured on matrices with different elastic moduli (measured by Image J). Mean ± SEM. n=40-50 per group, *P<0.05.

Figure 5.

Relaxin induces COX-2/PGE$_2$ in a stiffness-dependent manner. (A) Immunofluorescent staining of tracheal cross-sections; scale bar = 212 μm; n=3-10 per group with at least 10 tissue sections per animal. (B) Immunoblots of normal lung fibroblast lysates. Cells were plated on matrices with different elastic moduli and were treated without (Cntrl) and with relaxin (Rlxn); results were from at least 3 independent experiments. The graph represents quantification of the immunoblot by densitometry; Mean ± SEM. (C) Normal human lung fibroblasts were cultured on matrices with Young's elastic moduli of 0.5, 1, 2, 4, 12, 25 kPa, and treated with or without relaxin. Supernatants of cells were collected and PGE$_2$ concentrations were detected by PGE$_2$ enzyme-linked immunosorbent assay; Mean ± SEM, n=5-10 per group. *P<0.05.
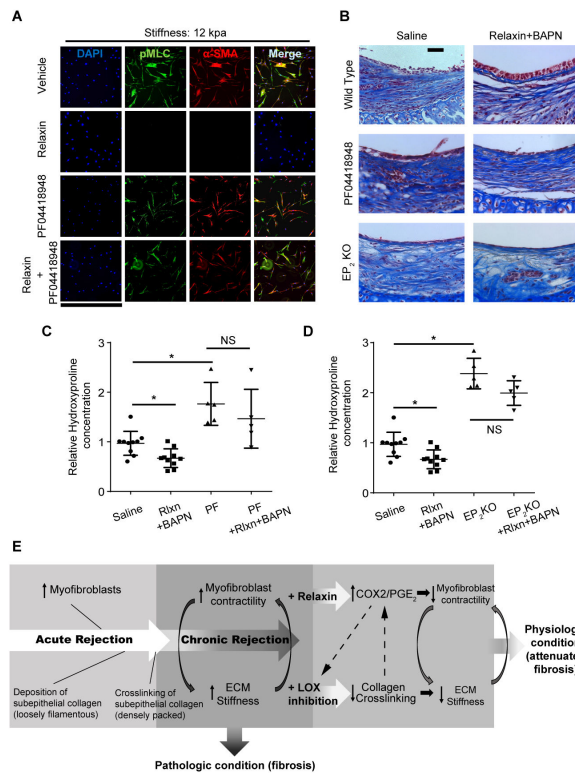
Figure 6.

PGE$_2$ inhibition abrogates the beneficial effects of relaxin and BAPN combined treatment. (A) Immunofluorescent staining of lung fibroblasts cultured on matrices with Young's elastic moduli of 12 kPa. Cells were treated with DMEM only, relaxin, PF-04418948 (EP$_2$ antagonist), or PF-04418948 with relaxin. Results are from at least 3 independent experiments; scale bar = 848 μm. (B) Representative images of Masson trichrome staining of tracheal cross-sections; scale bar = 50 μm; n=3-10 per group with at least 10 tissue sections per animal. (C, D) Hydroxyproline concentration in tracheal hydrolysates relative to controls was measured to assess the amount of collagen. Mean ± SD. PF= PF-04418948. *P<0.05, Tukey's test was used as post hoc test. (E) At the end of acute rejection, there is infiltration of myofibroblasts that deposit collagen. Crosslinking of loose collagen is catalyzed by LOX to form densely packed fibers that increase ECM stiffness. Fibrotic ECM stiffness may then activate cells to be more contractile leading to further collagen deposition. This positive feedback loop leads to persistent fibrosis and creates a pathologic condition. Relaxin upregulates COX-2/PGE$_2$, decreasing cellular contraction, which in turn, promotes ECM softening. LOX inhibition downregulates collagen cross-linking, thereby, decreasing ECM stiffness which in turn, decreases myofibroblast contractility. This breaks the positive feedback loop and returns the tissue to a physiologic condition. Furthermore, COX-2/PGE$_2$ may contribute to further decrease collagen cross-linking and ECM softening through inhibiting LOX. A soft ECM may also increase COX-2/PGE$_2$, which in turn, can decrease myofibroblast contractility. These mechanisms may further support the reversal of fibrosis.